Northumbria Research Link

Northumbria University
NEWCASTLE

University**Library**

Article

Bio-inspired synthesis of reduced graphene oxide wrapped Geobacter sulfurreducens as a hybrid electrocatalyst for efficient oxygen evolution reaction

Shafeer Kalathil, Krishna P. Katuri, Amira S. Alazmi, Srikanth Pedireddy, Nikolay Kornienko, Pedro M. F. J. Costa, and Pascal E. Saikaly

Chem. Mater., **Just Accepted Manuscript** • DOI: 10.1021/acs.chemmater.9b00394 • Publication Date (Web): 17 Apr 2019

Bio-inspired synthesis of reduced graphene oxide wrapped *Geobacter sulfurreducens* as a hybrid electrocatalyst for efficient oxygen evolution reaction

Shafeer Kalathil[1], Krishna P. Katuri[1], Amira S. Alazmi[2], Srikanth Pedireddy[1], Nikolay Kornienko[3], Pedro M. F. J. Costa[2], Pascal E. Saikaly[1]*

[1]*Division of Biological and Environmental Sciences & Engineering, Water Desalination and Reuse Center, King Abdullah University of Science and Technology, Thuwal, Saudi Arabia 23955-6900*

[2]*Division of Physical Sciences and Engineering, King Abdullah University of Science and Technology, Thuwal, Saudi Arabia 23955-6900*

[3]*Department of Chemistry, Université de Montréal, Roger-Gaudry Building, Montreal, Quebec, H3C 3J7, Canada*

** To whom correspondence should be addressed.* E-mail: pascal.saikaly@kaust.edu.sa

Abstract

Doping/decorating of graphene or reduced graphene oxide (rGO) with heteroatoms provides a promising route for the development of electrocatalysts useful in many technologies, including water splitting. However, current doping approaches are complicated, not eco-friendly and not cost-effective. Herein, we report the synthesis of doped/decorated rGO for oxygen evolution reaction (OER) using a simple approach that is cost-effective, sustainable and easy to scale up. The OER catalyst was derived from the reduction of GO by an exo-electron transferring bacterium, *Geobacter sulfurreducens*. Various analytical tools indicate that OER active elements such as Fe, Cu, N, P, and S decorate the rGO flakes. The hybrid catalyst (i.e., *Geobacter*/rGO) produces a geometric current density of 10 mA cm^{-2} at an overpotential of 270 mV vs. the reversible hydrogen electrode (RHE) with a Tafel slope of 43 mV dec^{-1}, and possesses high durability, evidenced through 10 hours of stability testing. Electrochemical analyses suggest the importance of Fe and its possible role as active site for OER. Overall, this work represents a simple approach towards the development of earth-abundant, eco-friendly and highly active OER electrocatalyst for various applications such as solar fuel production, rechargeable metal-air batteries, and microbial electrosynthesis.

Introduction

The world is facing a rapidly growing demand for energy. Currently, energy production depends mainly on fossil fuels,[1] which are being rapidly depleted and are a major cause of climate change. Hence, there is a need to explore alternative energy sources where the renewable sources stand out as the most attractive.[1] Amongst these, electrons extracted from water via water oxidation can be used to make molecular hydrogen or high-value chemicals/fuels from carbon dioxide (CO_2) reduction.[2]

Water splitting is a key process in solar fuel production,[3] rechargeable metal-air batteries,[4] and microbial electrosynthesis.[5-7] One of the main challenges in water splitting is that water oxidation needs a high energy input due to its kinetically sluggish multi-step reaction pathway.[8] Hence, stable, highly active and low-cost water oxidation catalysts should be developed for the wide-scale application of this process for energy production. Currently, metal oxide-based compounds such as IrO_2 and RuO_2 show the highest water oxidation activities with low overpotential at 10 mA cm^{-2}.[8] However, these materials suffer from multiple disadvantages such as scarcity, high cost and poor stability.[8] Due to their relatively high conductivity, mechanical stability, widespread availability and low toxicity, graphene flakes bear great promise for electrocatalytic purposes.[8, 9] Whilst the catalytic performance of exfoliated graphene is poor, it can be improved through functionalization with hetero-elements to create highly active catalytic sites.[9] Recently, the doping/decorating of graphene with non-metals (e.g., S, N, P, F and O)[9-13] and metals[8] (e.g., Fe and Ni) has proven to be a feasible strategy to render it an efficient electrocatalyst for oxygen evolution reaction (OER), hydrogen evolution reaction (HER) and oxygen reduction reaction (ORR). In the case of graphene doping with nitrogen (N-graphene),[9] the substitutional element influences the spin density and charge distribution in the adjacent carbon atoms. Overall, this creates an "activation region" on the graphene surface which can

subsequently participate in various catalytic reactions.[14, 15] There are several ways to produce N-graphene materials through direct and post-synthesis methods[9] (summarized in Table S1).

Sulfur (S) and phosphorous (P) are other elements that can be introduced into graphene.[10, 13] As their size and electronegativity are largely different from carbon, these elements can induce structural distortions and locally change the electronic structure of graphene. In the presence of a precursor containing S, the chemical vapor deposition (CVD) approach can be used to produce S-doped graphene (S-graphene).[9] P-doped graphene (P-graphene) can be prepared by treating graphene oxide (GO) with phytic acid at high temperature.[10] The doping of graphene with several elements at the same time, as for example, doping with N and S or N, S and P can further enhance the catalytic activity due to synergetic effects. [12, 16, 17] While not exhaustive, the above-mentioned strategies represent the most common approaches to produce doped graphene. Generally, these methods suffer from multiple drawbacks such as high cost, use of complicated synthesis procedures (high temperature and use of gases) and toxic precursors, and the release of hazardous waste-products (Table S1).

Green synthesis of reduced GO (rGO) from GO has been demonstrated using pure cultures of extracellular electron transfer (EET)-capable bacteria, such as *Shewanella oneidensis* MR-1,[18, 19] *Bacillus subtilis* 168,[20] *Gluconobact roseus,*[21] and *Desulfovibrio desulfuricans*.[22] EET-capable bacteria have the ability of coupling the oxidation of substrates (electron donor) in their cytoplasm with the reduction of insoluble extracellular electron acceptors for respiration. The molecular mechanism of electron transfer to GO by EET-capable bacteria was only reported by few studies, where electron transfer to GO was mediated either directly by outer membrane cytochromes as in *Shewanella oneidensis* MR-1[18, 19] or indirectly by redox mediator (e.g., vitamin K_3) as in *Bacillus subtilis* 168.[20] The reduction of GO to rGO was also been reported using mixed-culture inoculum such as anaerobic

sludge,[23] river water,[24] water channel sediment and paddy soil,[24] with the main objective to demonstrate the applicability of GO for the selective enrichment of EET-capable bacteria from the environment.

As living organisms, bacteria are mainly composed of carbon (50% on dry weight basis) with abundant heteroatoms (e.g., N, P, and S) and trace elements.[25] Therefore, bacteria can provide abundant heteroatoms to dope carbon materials. The production of carbon dot-heteroatom (N, S, and P) doped rGO for ORR was recently been demonstrated in a two-step process using the EET-capable bacterium *S. oneidensis* MR-1, where GO is reduced to rGO by *S. oneidensis* MR-1 in the first step followed by hydrothermal treatment at 180 °C in the second step.[26]

Inspired by these studies, here we developed an eco-friendly and highly efficient OER catalyst by utilizing for the first time the EET capability of the non-pathogenic bacterium, *Geobacter sulfurreducens*, to convert GO to rGO while simultaneously doping/decorating graphene with non-metallic (N, S and P) and transition metal species (Fe and Cu) derived from *G. sulfurreducens* in a single step. The rationale for selecting *G. sulfurreducens* is because it is commonly detected as a dominant member of anodic community in microbial electrochemical systems due to its outstanding performance in generating electricity (using conductive electrodes as electron acceptor) through substrate oxidation.[27, 28] The unique ability of *G. sulfurreducens* to make contact with insoluble electron acceptors is because it possesses a vast network of multi-haem containing outer-membrane c-type cytochromes (OM c-Cyts) and nano-filaments (known as microbial protein nanowires).[27, 29] It employs OM c-Cyts to transfer metabolically generated electrons from its periplasm to the cell exterior through a well-orchestrated EET process.[30] Iron is a key component of haem group in c-Cyts. The content of iron in *G. sulfurreducens* cell is three-fold higher compared to *Escherichia coli*, which is the best bacteria reported in terms of iron assimilation.[31] This is mainly due to the fact that *G.*

sulfurreducens possesses the highest number of genes coding for c-Cyts (111 in the whole genome).[32] Thus, this bacterium assimilates more iron into their cell for synthesizing c-Cyts required for EET mechanism. Moreover, in a recent study it was shown that iron and not nickel was performing water-splitting in a catalyst made of layers of nickel and iron.[33] In addition to c-Cyts, *G. sulfurreducens* possesses multicopper containing proteins[34] and Fe-S protein clusters[30]. Taken together, these characteristics make *G. sulfurreducens* ideally suited for generating metal and non-metal doped/decorated rGO for electrocatalysis such as OER.

The synthesis protocol of doped/decorated rGO using *G. sulfurreducens* overcomes most drawbacks of other existing methods aimed at the production of doped/decorated graphene for electrocatalysis (Table S1). The hybrid catalyst (i.e., *Geobacter*/rGO) demonstrated high electrocatalytic activity towards OER in alkaline electrolyte, producing a geometric current density of 10 mA cm^{-2} at an overpotential of 270 mV vs. the reversible hydrogen electrode (RHE).

Experimental Procedures

Synthesis of graphene oxide (GO) and hydrothermally reduced graphene oxide (HrGO):

Graphite powder (Alfa Aesar, <50 μm) was first oxidized using the so-called Improved-Hummers' method.[35] Typically, 3 g of graphite powder (Alfa Aesar) was added to a mixture of 360 mL H_2SO_4 (Sigma Aldrich, 99%) and 40 mL H_3PO_4 (Sigma Aldrich, 85 wt %). This was followed by the slow addition of 18 g of $KMnO_4$ (Acros, 99%), taking care that the reaction temperature was maintained at <20 °C. Then, the resulting suspension was heated, in an oil bath, to 50 °C and stirred for 12 h. The coluor of the mixture turned from black to mud-brown. The reaction was allowed to cool to room temperature and treated with 400 mL of cold deionized water plus 3 mL of H_2O_2 (Sigma Aldrich, 30%). Then, the product was diluted with deionized water to a total volume of 2 L. Finally, the

suspension was repeatedly washed with water and centrifuged (Hettich U320, 9000 rpm, 10 min) until the pH was nearly neutral. At this point, the suspension was vacuum dried in the centrifuge tubes (60 °C, 12 h) and the resulting powder collected. The graphene oxide (GO) solution (5 mg ml^{-1}) was prepared by dispersing the GO powder in deionized water and then the mixture was stirred for 24 hours. Hydrothermally reduced graphene oxide (HrGO) was prepared according to a previous report.[36]

Reduction of GO to reduced graphene oxide (*Geobacter*/rGO) by *G. sulfurreducens*: *G. sulfurreducens* PCA (ATCC 51573) was used as the bacterium for the synthesis of *Geobacter*/rGO. *G. sulfurreducens* was cultured in an anaerobic serum bottle using acetate (20 mM) as electron donor and fumarate (50 mM) as the electron acceptor in defined media.[37] The entire culturing was conducted in an anaerobic glove box and the bottle was then kept in a shaking incubator (30 °C) for five days. Although strict anaerobic conditions are not required as *G. sulfurreducens* can survive in oxic environments,[38] we maintained anaerobic conditions for the experiment to avoid electron consumption by oxygen which may interfere in the GO reduction.

As grown *G. sulfurreducens* suspension (100 ml) having an optical density (OD) of 0.8 was centrifuged and the resulting pellet appeared red in colour due to the presence of multi-heme containing outer-membrane c-type cytochromes (OM c-Cyts).[39] The bacterial pellet was added to an anaerobic serum bottle that contains *G. sulfurreducens* growth media (100 ml, except fumarate) with 20 mM acetate (electron donor) and GO (0.4 mg mL^{-1}) as the sole source of electron acceptor. The bottle was kept in a temperature-controlled room (30 °C) for 2 days without shaking. Several batch experiments were conducted to reproduce the data. Three serum bottles were kept under similar conditions but without inoculation of *G. sulfurreducens* (denoted as abiotic GO). To understand the role of OM c-Cyts in the GO reduction, *G. sulfurreducens* was grown with a medium containing 30

μM of the iron chelator, 2,2'-bipyridine to suppress the production of OM c-Cyts.[40] The cells grown with bipyridine were then employed for the GO reduction. Heat-killed bacteria were prepared by autoclaving bacterial solution. The autoclaved bacterial cells were used as the inoculum to reduce GO to understand the metabolic activity of bacteria in the GO reduction.

***Geobacter*/rGO and abiotic GO processing:** After two days of *G. sulfurreducens* incubation with GO, a dark colored hydrogel type *Geobacter*/rGO was precipitated at the bottom of the bottle. The solution underwent centrifugation (8000 rpm, 6 minutes) to collect the *Geobacter*/rGO material. The material was washed six times with MilliQ water by gentle vortexing to remove any media contribution on the *Geobacter*/rGO. After the washing process, *Geobacter*/rGO was kept in an oven (45 °C) overnight for drying the sample. The dried sample was used for all experiments. There was no GO reduction in the absence of G. sulfurreducens under similar conditions even after 2 days of the incubation (abiotic GO). The abiotic GO was collected by centrifugation (14000 rpm, 10 minutes) and the collected sample was washed with MilliQ water (6 times) to remove any possible media contribution in the sample. The collected abiotic GO sample was dried at 45 °C in an oven overnight for drying. The dried abiotic GO sample was used for all the experiments.

Materials Characterization: The elements are quantified using an ICP-OES Varian 720-ES Spectrometer equipped with a dual detector assembly that covered a wavelength from 165 to 782 nm. Raman spectra were collected using a WITec Alpha300RA spectrometer at an excitation wavelength of 488 nm. The survey and high-resolution X-ray photoelectron spectroscopy (XPS) spectra were obtained at fixed analyzer pass energies of 160 eV and 20 eV, respectively (Model: ESCA 3400). Transmission electron microscopy (TEM) images were acquired in bright-field mode with a Phillips Tecnai F20 electron microscope with 200 kV accelerating voltage. Samples were prepared by

sonicating in ethanol and drop-casting on an ultrathin carbon grid, followed by drying under ambient conditions. Contact angle was measured using a FTA1000 B Class goniometer (First Ten Ångstroms), paired with FTA32 software. Scanning electron microscopy (SEM) images were acquired using a Zeiss Merlin microscope under an acceleration voltage of 5 keV. The SEM-EDS measurements were obtained by using an Oxford EDS X-Max SDD detector attached to the Zeiss Merlin scanning electron microscope, and the AzTecEnergy EDS analysis software. Fourier-Transform Infrared (FTIR) spectra were obtained by a Thermo Scientific™ Nicolet™ iS50 FTIR Spectrometer at ATR mode.

Electrochemical tests: The activity of the *Geobacter*/rGO towards the OER was tested using a rotating disc electrode (RDE). The working electrode was prepared by the following procedure: first, the *Geobacter*/rGO material (~2 mg) was dispersed in 500 µl of ethanol, 500 µl of water and 15 µl of Nafion (as binder). The dispersed solution was sonicated for 30 min. 2 µl of the obtained slurry was drop-coated onto a 3 mm glassy carbon disc electrode (GCE; loading concentration ~ 0.05 mg cm^{-2}) and dried under a lamp for 1 h. The same procedure and loading concentration were used to make working electrodes with hydrothermally reduced GO (HrGO), abiotic GO and pure *G. sulfurreducens* dried cells. The electrochemical measurement was carried out using a BioLogic VMP3 electrochemical working station in 1 M KOH (Sigma Aldrich, semiconductor grade, pellets, 99.99% trace metals basis) at room temperature using a three-electrodes system, in which Pt coil and Mercury/Mercury oxide (Hg/HgO) were used as counter and reference electrodes, respectively. Linear sweep voltammetry (LSV) experiments were performed at a scan rate of 5 mV s^{-1} while maintaining a constant rotational speed of 1600 rpm. Stability test for the *Geobacter*/rGO OER catalyst was performed by conducting chronoamperometry measurement (CA) at an overpotential of 270 mV vs. reversible hydrogen electrode (RHE) under a constant rotating speed of 1600 rpm. Cyclic voltammetry

(CV) analysis was conducted at a scan rate of 5 mV s^{-1} without rotation. Electrochemical impedance spectroscopy (EIS) measurements were performed for the *Geobacter*/rGO in 1 M KOH from 1000 kHz to 100 mHz. All the measured potentials vs. the Hg/HgO were converted to RHE by the Nernst equation ($E_{RHE} = E_{Hg/HgO} + 0.0591\ pH + 0.140$). All the experiments were done at least in triplicates to reproduce the data.

Results and discussion

An active culture of *G. sulfurreducens*, with acetate (20 mM) as the electron donor and GO (0.4 g L^{-1}) as the electron acceptor, was used (Fig. 1a). The culture was incubated under anaerobic conditions for 2 days at 30 °C to permit the complete reduction of the brownish GO and formation of a black hydrogel (lower inset in Fig. 1c). The formation of a hydrogel was previously reported for a pure culture of *Geobacter* sp. strain R4 when cultivated with acetate and GO (0.67 g L^{-1}) at 28 °C; however it required a longer incubation period (30 d) to form a hydrogel. In contrast, hydrogel formation was not observed with other EET-capable bacteria such as *Shewanella oneidensis* MR-1, *Bacillus subtilis* 168, *Gluconobact roseus*, or *Desulfovibrio desulfuricans* when incubated with GO (0.2-0.5 g L^{-1}) under anaerobic conditions for 1 day[20, 22] or 3 days.[18]

Control experiments were done under similar conditions but in the absence of *G. sulfurreducens* (herewith termed abiotic GO; see details in Supporting Information). These control experiments confirmed that there was no reduction of GO without *G. sulfurreducens* in the solution. We employed scanning electron microscopy (SEM) to investigate the morphology of the as prepared *Geobacter*/rGO hydrogel. SEM images demonstrated that the *Geobacter* cells were embedded in the crosslinked ultrathin sheets of rGO matrix. Moreover,

Geobacter cells were wrapped with rGO sheets indicating strong interaction between *Geobacter* and rGO sheets (Fig. 1c). The dimensions of the cells in the *Geobacter*/rGO hydrogel are in accordance with the size of *Geobacter* cells (Fig. 1b).

To understand the role of OM c-Cyts in the reduction of GO, we suppressed the production of OM c-Cyts by adding bipyridine (an iron-chelator) in the *G. sulfurreducens* growth media. Bipyridine is known to shut down the production of Cyts by chelating with iron.[40] Inductively coupled plasma optical emission spectrometry (ICP-OES) analysis showed significantly lower Fe in the supressed cells compared to unsuppressed cells (Fig. S1). The OM c-Cyts suppressed cells did not reduce GO (Fig. S2) suggesting that OM c-Cyts are essential for GO reduction by *G. sulfurreducens*. Also, heat-killed bacteria were not able to reduce GO. This observation indicates that the *G. sulfurreducens* physiological activity was responsible for the reduction of GO as the electrons generated metabolically, via acetate oxidation, were transferred extracellularly to GO (which acts as the terminal electron acceptor) by OM c-Cyts, reducing it to rGO.

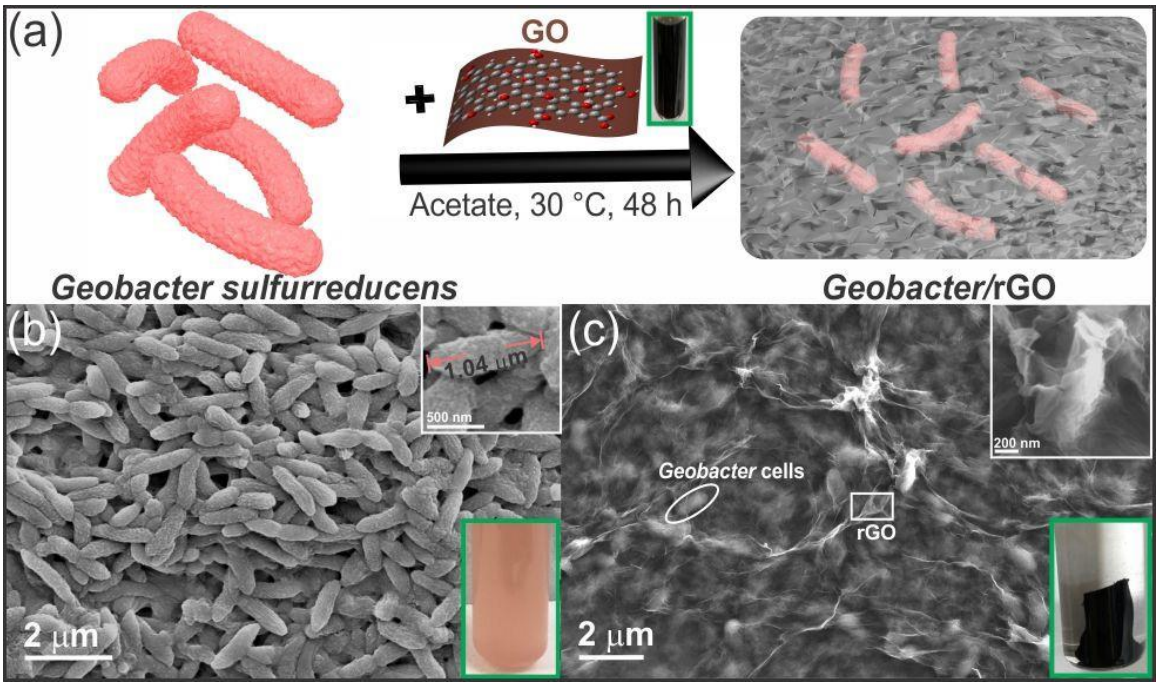

Figure 1. Schematic illustration and morphological characterization. (a) Schematic illustration for the reduction of graphene oxide (GO) by *G. sulfurreducens* (conditions: 30 ^{0}C, anaerobic, pH 7).

(b) Low and high magnification (upper inset) Field-Emission Scanning Electron Microscope (FE-SEM) images of dried *G. sulfurreducens* cells and a digital photograph of the suspended *G. sulfurreducens* cells (lower inset). The red color is due to the iron-rich content in *G. sulfurreducens*. (c) Low and high magnification (upper inset) FE-SEM images of *Geobacter*/rGO and a digital photograph of the *Geobacter*/rGO hydrogel (lower inset) at the bottom of the anaerobic serum vial after 48 h of incubation.

Additional evidence for the successful reduction was acquired through spectroscopic observations (Fig. 2). We thoroughly investigated the *Geobacter*/rGO sample in comparison to GO using X-ray photoelectron spectroscopy (XPS) analysis. The high resolution C1S spectra of the *Geobacter*/rGO and abiotic GO (Fig. 2a) were significantly different, with the C=C peak being clearly dominant in the former. The C/O atomic ratio in *Geobacter*/rGO and abiotic GO were calculated to be 5.5 and 2.78, respectively (Figure S3 and S4). The increased C/O ratio in *Geobacter*/rGO confirmed the successful reduction of GO by *G. sulfurreducens*. After the GO reduction, the *Geobacter*/rGO showed presence of nitrogen (5%) (Fig. 2c and Fig. S3) which may be derived from *G. sulfurreducens* (Fig. S5). Further confirmation was provided by Raman analysis. In the Raman spectra of abiotic GO and *Geobacter*/rGO (Fig. 2d), the D band is considerably narrower in *Geobacter*/rGO and the set of peaks at higher wavenumber (2500-3500 cm^{-1}) were more resolved. The I_D/I_G ratio of *Geobacter*/rGO (1.18) was higher than that of abiotic GO (0.93). The increased I_D/I_G ratio implies that there are less in-plane sp^2 bonds and more out of plane sp^3 bonds in the carbon atoms within the material, which may originate from the inclusion of the dopants.[41] On the other hand, the increased peak intensity in the high wavenumber region, corresponding to the 2D, D + G and 2G bands may indicate a higher degree of disruption of the graphitic AB stacking order in *Geobacter*/rGO.[42] Also, the G band of *Geobacter*/rGO blue-shifted possibly due to defects or N-doping by *G. sulfurreducens* (Fig. 2d) (Fig. 2d).[43] Taken together, these results confirm the modulation of GO by *G. sulfurreducens*.

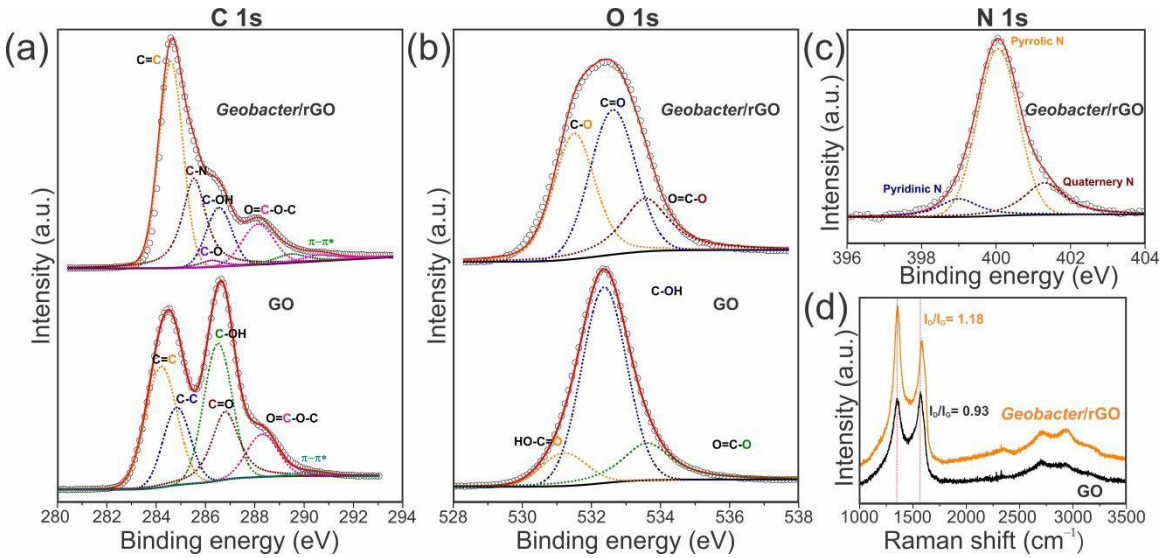

Figure 2. Comparative X-ray photoelectron spectroscopy (XPS) and Raman spectra of GO vs. *Geobacter*/rGO. Fitted XPS spectra of GO vs. *Geobacter*/rGO for (a) C 1s region, (b) O 1s region, and (c) N 1s region. (d) Raman spectra of GO and *Geobacter*/rGO.

Transmission electron microscopy (TEM) was utilized to examine the chemical and structural nature of *Geobacter*/rGO (Fig. 3). The low magnification TEM image of *Geobacter*/rGO clearly demonstrated the formation of interlinked network of rGO with embedded *Geobacter* cells (Fig. 3a). Presumably, the majority of the iron species are in the form of small clusters or in an amorphous phase. However, iron oxide (FEO) nanoparticles were occasionally seen (Fig. 3b). The lattice spacing, calculated from the Fast Fourier Transform (FFT) image, of 1.3 and 1.1 Å is close to FeO (111) and (200) planes (lower inset of Fig. 3b). The inverse of the FFT is overlaid atop the original image to highlight the FeO particle. The *Geobacter*/rGO consisted of primarily single to few-layer morphology (Fig. 3c-d). The interlayer spacing between the individual sheets shrunk from 4.5 Å for the GO precursor (Fig. S6b) to 3.6 Å (Fig. 3e), pointing to the reduction of GO to *Geobacter*/rGO. The FFT reconstruction of the *Geobacter*/rGO illustrates the honeycomb carbon lattice, as expected for rGO (Fig. 3f).

Multiple points of evidence indicated that the *Geobacter*/rGO was doped/decorated with elements beneficial for efficient OER. The ICP-OES analysis of *G. sulfurreducens* cells revealed that this bacterium was abundant with S, P, Fe and Cu (Table S2). The ICP-OES analysis of the *Geobacter*/rGO also showed the presence of these elements which may be derived from *G. sulfurreducens* (Table S2). XPS analysis showed 11.9 % N (wt. %) in the pure *G. sulfurreducens*, 5 % N in the *Geobacter*/rGO and no N in pure GO (Fig. S3, S4 and S5). It should be noted that S, P, Fe, Cu and N are excellent candidates for the OER. [17, 44-46]

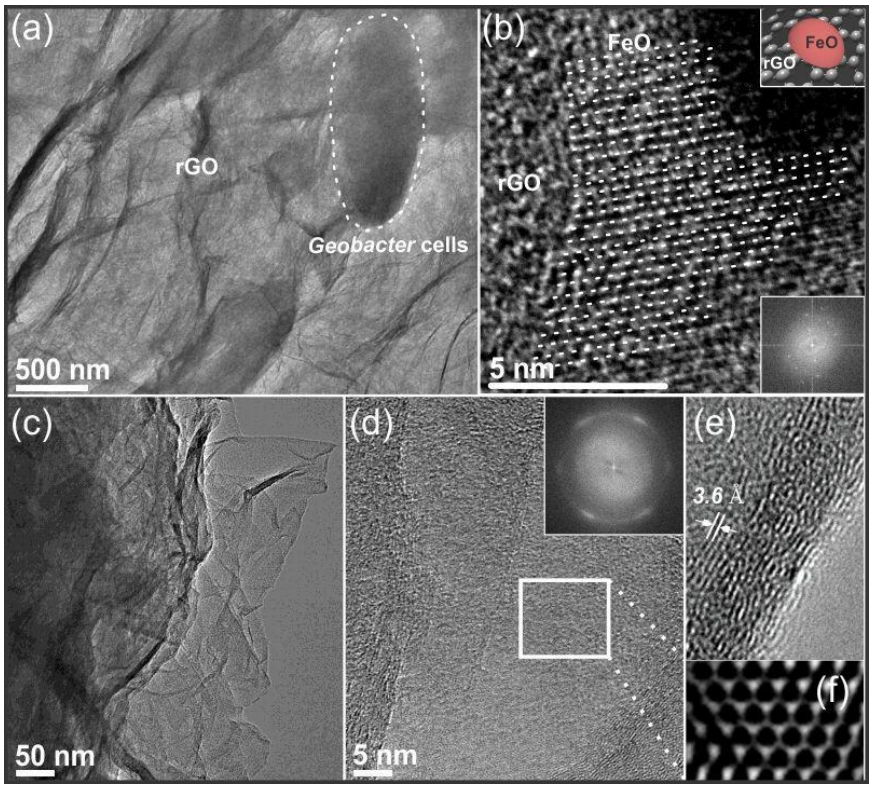

Figure 3. Structural characterizations of *Geobacter*/rGO using transmission electron microscopy (TEM). (a) TEM image of *G. sulfurreducens* cells embedded in rGO. (b) High-resolution TEM image and Fast Fourier Transform (FFT) pattern of rGO-FeO demonstrate the crystalline FeO. (c, d) Bright field TEM reveals single- to few-layer morphology of the *Geobacter*/rGO. The FFT inset of the single layer *Geobacter*/rGO illustrates the hexagonal arrangement of the carbon lattice. (e) A magnified image of several stacked *Geobacter*/rGO sheets reveals an interlayer spacing of ~3.6 Å,

pointing to a near-complete reduction of the GO precursor. (f) An inverse FFT of single *Geobacter*/rGO sheet showing the honeycomb carbon lattice.

After thoroughly characterizing the *Geobacter*/rGO, the electrocatalytic OER properties of *Geobacter*/rGO were evaluated using linear sweep voltammetry (LSV) (Fig. 4). To validate and compare its OER activity, control experiments were performed utilizing hydrothermally reduced graphene oxide (HrGO)[36] and abiotic GO. Working in 1M KOH electrolyte, the *Geobacter*/rGO exhibited some OER activity while the other electrodes (built from HrGO and abiotic GO) showed minimal OER currents (Fig. 4a). Chronoamperometry (CA) experiments illustrated that the OER current generated by the *Geobacter*/rGO gradually increased, stabilising after ~20 h (Fig. 4b). By contrast, there was no current produced with the HrGO and abiotic GO samples using similar mass loadings of 0.05 mg cm^{-2} (Fig. 4b). The *Geobacter*/rGO reached the highest OER performance with an overpotential of 270 mV (vs. RHE) to produce a geometric current density of 10 mA cm^{-2} (Fig. 4c). The Tafel slope of 43 mV dec^{-1} for *Geobacter*/rGO (Fig. 4d) is amongst the best for alkaline OER catalysts.[47] The stark differences in Tafel slopes between the abiotic GO and *Geobacter*/rGO point to significant differences in per-site catalytic activity. There was no change in the OER activity of the *Geobacter*/rGO even after changing the used electrolyte for a fresh one (Fig. S7). The electrocatalytic inertness of HrGO and abiotic GO (even after the CA experiment) added to the absence of a significant change in the OER activity of the *Geobacter*/rGO after changing the electrolyte, rules out any possible role of impurities or platinum dissolution from the counter electrode. Also, impurities were not detected in the KOH (semiconductor grade) supporting electrolyte (Table S2) avoiding any possible electrolyte contamination during electrochemical experiments. Moreover, we did not observe any heteroatoms in the electrolyte after the CA experiment which confirms the robustness of the

doped/decorated elements originated from the *Geobacter*/rGO (Table S2). The OER activity measured for the *Geobacter*/rGO is therefore solely attributed to this material. The low overpotential of 270 mV demonstrates the OER activity of *Geobacter*/rGO is much higher than that of recently reported electrocatalysts and benchmark metal oxides such as IrO_2 and RuO_2 catalyst (Table S3). In addition, *Geobacter*/rGO catalyst was stable even after 10 hours of CA experiment (Fig. 4e). Control experiments performed with pure *G. sulfurreducens* cells showed negligible OER activity, even after an equivalent CA experiment (Fig. S8). As previously mentioned, multiple sources of evidence (Table S2 and Fig. 2c) demonstrate that the *Geobacter*/rGO was doped/decorated with species promoting the high OER activity of *Geobacter*/rGO electrocatalyst. In the *Geobacter*/rGO OER catalyst, *G. sulfurreducens* provided necessary OER elements to the rGO support which is distinct from HrGO and other rGO produced by various methods. To investigate the origin of this high activity in *Geobacter*/rGO electrocatalyst, we washed *Geobacter*/rGO sample with 1 M HCl solution to remove cell debris, organic matter and transition metals (such as Fe) as corresponding chlorides. Interestingly, acid washing diminished the catalytic activity of *Geobacter*/rGO electrocatalyst (Fig. 4c-d) indicating that *Geobacter* cells are crucial for attaining such a high catalytic performance.

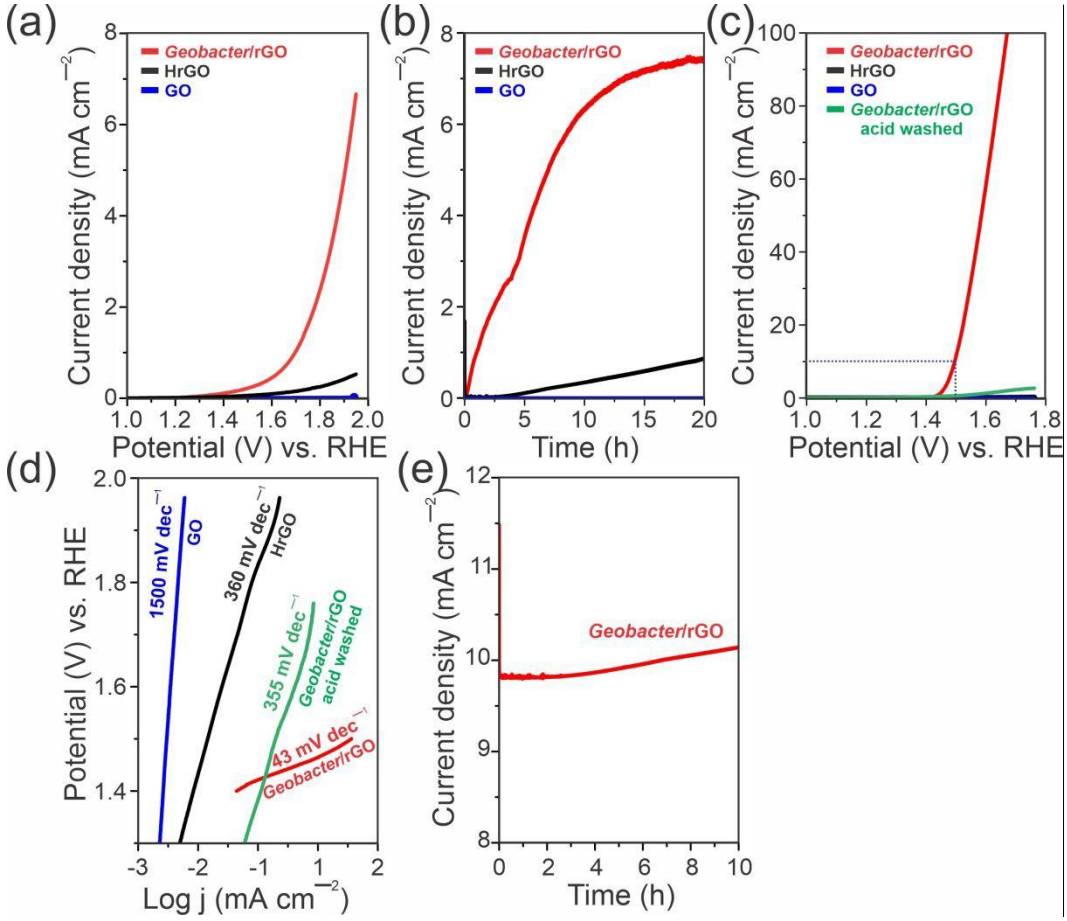

Figure 4. Electrochemical oxygen evolution reaction (OER) performance of GO, *Geobacter*/GO and HrGO deposited glassy carbon electrodes in 1M KOH (pH ~ 14) solution. (a) Linear sweep voltammetry (LSV) plots normalized to geometric area of electrodes before chronoamperometry experiment at a scan rate of 5 mV s^{-1}, (b) Chronoamperometry plots at an applied potential of 1.5 V vs RHE, (c) LSV plots after chronoamperometry experiment at a scan rate of 5 mV s^{-1}, (d) Tafel plots of the used catalysts and (e) Stability test for *Geobacter*/rGO OER catalyst at an overpotential of 270 mV in 1M KOH. The rotating speed for all experiments was kept as 1600 rpm.

We performed several experiments to decipher the enhanced OER activity of *Geobacter*/rGO catalyst after the CA. SEM image of *Geobacter*/rGO catalyst after the CA showed the formation of several nanoparticles on the surface of the catalyst (Fig. 5a). A line-profile analysis using energy-dispersive spectroscopy (EDS) confirmed that these particles are made of FeO (Fig. 5b). The direction of the EDS line scan is denoted by a white arrow across the nanoparticle. The profile analysis indicates that Fe and oxygen atoms are distributed uniformly throughout the particle. Moreover, the intensity of

the Fe component was higher compared to oxygen, and also oxygen concentration at the rims of the nanoparticle was slightly higher, suggesting surface oxidation is responsible for the formation of FeO. ICP-OES analysis further confirmed that the hetero elements are intact with the catalyst even after the CA (Table S2). Also, the contact angle measurement and Fourier-transform infrared (FTIR) analysis showed that the *Geobacter*/rGO catalyst became more hydrophilic after the CA (Fig. 5c and 5d).

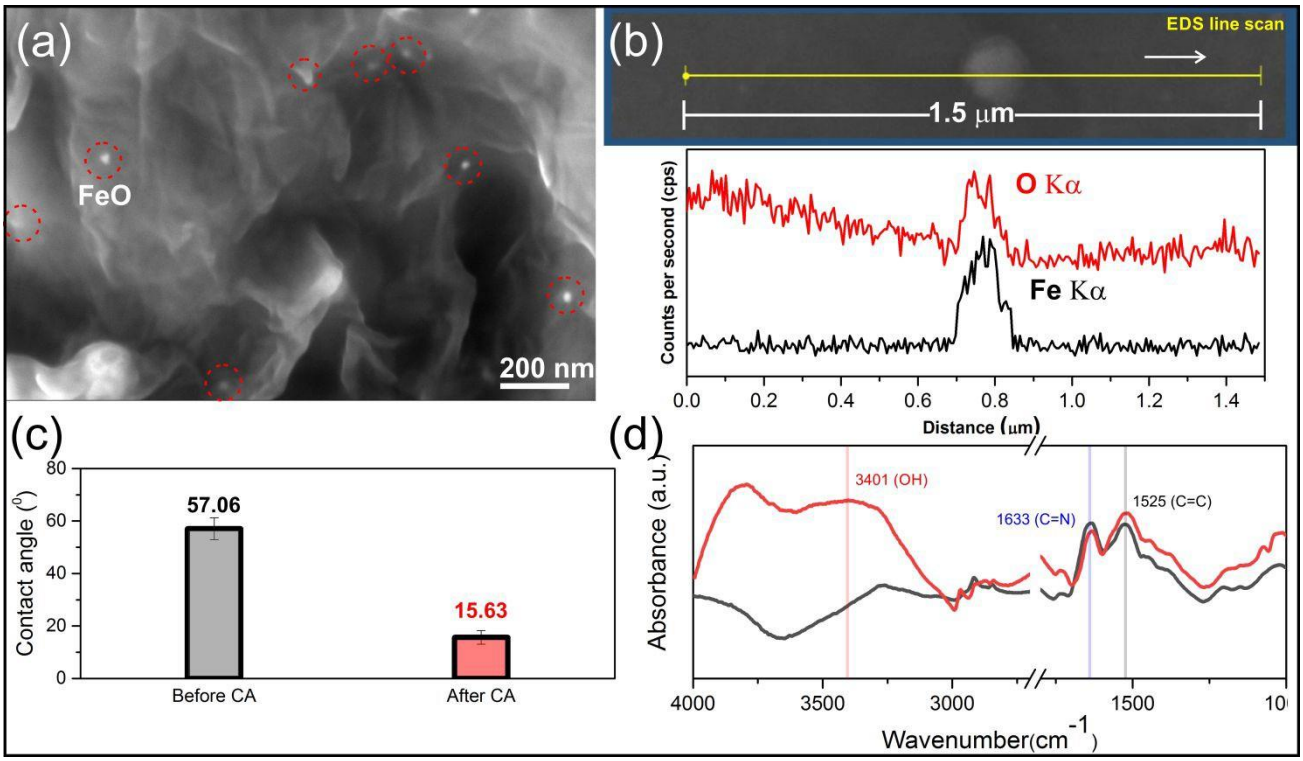

Figure 5. Scanning electron microscopy (SEM), Energy-dispersive spectroscopy (EDS), contact angle and Fourier-transform infrared (FTIR) characterization to evaluate changes in *Geobacter*/rGO catalyst after chronoamperometry (CA) measurement. (a) High magnification SEM image shows the presence of nanoparticles on the surface of *Geobacter*/rGO catalyst after the CA (b) EDS line profile analysis confirms that these nanoparticles are made of iron oxide (c) Contact angle and (d) FTIR spectroscopy measurement of *Geobacter*/rGO electrode before (black) and after (red) the CA.

Complementary electrochemical impedance spectroscopy (EIS) analysis was conducted on the *Geobacter*/rGO electrode before and after the CA. The impedance spectra (Fig. S9) were fitted using a standard Randles circuit with EC-Lab V11.12 (Bio-Logic). Based on the Randles circuit analysis, the charge transfer resistances (R_{ct}) were 10.3 (before CA) and 0.76Ω (after CA) for the tested *Geobacter*/rGO sample. This result demonstrates that the conductivity of *Geobacter*/rGO was significantly enhanced after the CA experiment. Furthermore, cyclic voltammetry (CV) plot of *Geobacter*/rGO, done after the CA, showed a reversible oxidation peak (Fig. S10). This redox peak likely corresponds to the oxidation of Fe (decorated on the *Geobacter*/rGO, Fig. 5a and 5b) into its catalytically active Fe(III) and Fe(IV) states because this peak occurs just prior of OER catalysis and corresponds to previous reports.[48] Note that the pair of redox peaks were absent in the corresponding CV before the CA (Fig. S10). The *Geobacter*/rGO exhibited a double-layer capacitance (C_{dl}) of 14.29 and 2.14 mF cm^{-2} after and before CA, respectively calculated from the CVs measured at non-Faradic region (Inset, Fig. S10). The enhanced C_{dl} suggests that electrochemical surface area (ECSA) of the *Geobacter*/rGO electrode after the CA was significantly enhanced indicating higher degree of accessibility of catalytic sites.

Catalyst wettability is crucial in heterogeneous catalysis. [49] Catalytic activity not only depends on the active sites, but also on the adsorption and desorption of the reactants and products. Hydrophilic surfaces can significantly improve catalysis by promoting a more catalytically favorable interaction between the electrode and electrolyte. A recent report proposed a strategy to enhance OER activity of NiFe hydroxide by simply improving surface hydrophilicity via phosphorylation. [50] Zhou et al. observed a gradual increase in the wettability of fluorine and nitrogen co-doped carbon microsphere electrode with continuous CV measurements which improved the electrode capacitance.[51] Such

observations demonstrate that continuous electrochemical measurements can facilitate electrode wettability and supports the enhanced wettability of *Geobacter*/rGO electrode after the CA. All the above results (Fig. 5, Fig. S9 and S10) showed that after the CA, the interaction between the electrolyte and *Geobacter*/rGO electrode greatly improved due to the increased ECSA and surface hydrophilicity on the electrode. Furthermore, the CA treatment opened the OER catalytic active sites to the electrolyte, evidenced by the appearance of a pair of redox peaks in the CV of *Geobacter*/rGO (Fig. S10). On the other hand, TEM and Raman analyses of the *Geobacter*/rGO electrode showed no morphological changes after the CA measurements (Fig. S11 and S12) demonstrating that the structural character of the *Geobacter*/rGO catalyst was largely unchanged.

Conclusions

In summary, we have successfully demonstrated a unique single step approach for synthesizing doped/decorated rGO by *G. sulfurreducens.* Further, we demonstrated that the resulting *Geobacter*/rGO worked efficiently as an OER electrocatalyst with an overpotential of 270 mV vs RHE producing a current density of 10 mA cm^{-2}. This overpotential of 270 mV is lower than those typically reported in studies using expensive benchmark metal oxide electrocatalysts such as IrO_2 and RuO_2. The approach used in this study is green and sustainable as it does not involve the use of toxic precursors and solvents. The OER activity observed in this report broadens the application of *G. sulfurreducens* as a cost-effective component of electrocatalyst manufacturing for large-scale energy conversion. Also, our work can inspire the use of other efficient EET-capable bacteria for synthesizing high-performing and low-cost electrocatalysts for various energy-related applications.

Acknowledgements

This work was supported by Competitive Research Grant (URF/1/2985-01-01) from King Abdullah University of Science and Technology (KAUST).

ASSOCIATED CONTENT

Supporting Information

The Supporting Information is available free of charge on the ACS Publications website. The Supporting Information contains the details of ICP-OES data (Table S2 and Fig. S1), XPS analysis (Fig. S3-5 and Fig. S13), HRTEM images (Fig. S6 and Fig. S11), electrochemical data (Fig. S7-10) and Raman data (Fig. S12).

AUTHOR INFORMATION

Corresponding Author

*Phone: (+966) 544700129; e-mail: pascal.saikaly@kaust.edu.sa

ORCID

Pascal Saikaly: 0000-0001-7678-3986

Authors Contributions

S.K, K.P.K and P.E.S. conceived the idea and designed the project. All the authors wrote the paper. S.K synthesized Geobacter/rGO, conducted electrochemical tests, FTIR and contact angle measurements. K.P.K. cultured bacteria. A.A produced GO and HrGO and performed ICP-OES and Raman. S.P performed and analyzed XPS, SEM, EDS, designed graphical abstract, TOC and schematic illustrations in Fig. 1, Fig.3, and Fig. S2. N.K. captured TEM and SEM. P.E.S and P.C. supervised the work. All authors discussed the results and commented on the manuscript.

Notes

The authors declare no competing financial interests.

References

1.Roger, I.; Shipman, M. A.; Symes, M. D., Earth-abundant catalysts for electrochemical and photoelectrochemical water splitting. *Nat. Rev. Chem.* **2017,** 1, (1).

2.Jung, S.; McCrory, C. C. L.; Ferrer, I. M.; Peters, J. C.; Jaramillo, T. F., Benchmarking nanoparticulate metal oxide electrocatalysts for the alkaline water oxidation reaction. *J. Mater. Chem. A* **2016,** 4, (8), 3068-3076.

3.Zhao, Y.; Swierk, J. R.; Megiatto, J. D., Jr.; Sherman, B.; Youngblood, W. J.; Qin, D.; Lentz, D. M.; Moore, A. L.; Moore, T. A.; Gust, D.; Mallouk, T. E., Improving the efficiency of water splitting in dye-sensitized solar cells by using a biomimetic electron transfer mediator. *Proc Natl Acad Sci U S A* **2012,** 109, (39), 15612-6.

4.Zheng, X.; Han, X.; Liu, H.; Chen, J.; Fu, D.; Wang, J.; Zhong, C.; Deng, Y.; Hu, W., Controllable Synthesis of Ni xSe (0.5 </= x </= 1) Nanocrystals for Efficient Rechargeable Zinc-Air Batteries and Water Splitting. *ACS Appl Mater Interfaces* **2018,** 10, (16), 13675-13684.
5.Bian, B.; Alqahtani, M. F.; Katuri, K. P.; Liu, D.; Bajracharya, S.; Lai, Z.; Rabaey, K.; Saikaly, P. E., Porous nickel hollow fiber cathodes coated with CNTs for efficient microbial electrosynthesis of acetate from CO2 using Sporomusa ovata. *J. Mater. Chem. A* **2018,** 6, (35), 17201-17211.
6.Katuri, K. P.; Kalathil, S.; Ragab, A. a.; Bian, B.; Alqahtani, M. F.; Pant, D.; Saikaly, P. E., Dual-Function Electrocatalytic and Macroporous Hollow-Fiber Cathode for Converting Waste Streams to Valuable Resources Using Microbial Electrochemical Systems. *Adv. Mater.* **2018,** 30, (26), 1707072.
7.Alqahtani, M. F.; Katuri, K. P.; Bajracharya, S.; Yu, Y.; Lai, Z.; Saikaly, P. E., Porous Hollow Fiber Nickel Electrodes for Effective Supply and Reduction of Carbon Dioxide to Methane through Microbial Electrosynthesis. *Adv. Funct. Mater.* **2018,** 28, (43), 1804860.
8.Cui, X.; Ren, P.; Deng, D.; Deng, J.; Bao, X., Single layer graphene encapsulating non-precious metals as high-performance electrocatalysts for water oxidation. *Energy Environ. Sci.* **2016,** 9, (1), 123-129.
9.Wang, H.; Maiyalagan, T.; Wang, X., Review on Recent Progress in Nitrogen-Doped Graphene: Synthesis, Characterization, and Its Potential Applications. *ACS Catal.* **2012,** 2, (5), 781-794.
10.Lai, J.; Li, S.; Wu, F.; Saqib, M.; Luque, R.; Xu, G., Unprecedented metal-free 3D porous carbonaceous electrodes for full water splitting. *Energy Environ. Sci.* **2016,** 9, (4), 1210-1214.
11.Qu, K.; Zheng, Y.; Dai, S.; Qiao, S. Z., Graphene oxide-polydopamine derived N, S-codoped carbon nanosheets as superior bifunctional electrocatalysts for oxygen reduction and evolution. *Nano Energy* **2016,** 19, 373-381.
12.Paraknowitsch, J. P.; Thomas, A., Doping carbons beyond nitrogen: an overview of advanced heteroatom doped carbons with boron, sulphur and phosphorus for energy applications. *Energy Environ. Sci.* **2013,** 6, (10).
13.Wang, J.; Ma, R.; Zhou, Z.; Liu, G.; Liu, Q., Magnesiothermic synthesis of sulfur-doped graphene as an efficient metal-free electrocatalyst for oxygen reduction. *Sci Rep* **2015,** 5, 9304.
14.Groves, M. N.; Chan, A. S. W.; Malardier-Jugroot, C.; Jugroot, M., Improving platinum catalyst binding energy to graphene through nitrogen doping. *Chem. Phys. Lett.* **2009,** 481, (4-6), 214-219.
15.Zhang, L.; Xia, Z., Mechanisms of Oxygen Reduction Reaction on Nitrogen-Doped Graphene for Fuel Cells. *The Journal of Physical Chemistry C* **2011,** 115, (22), 11170-11176.
16.Zhao, J.; Liu, Y.; Quan, X.; Chen, S.; Zhao, H.; Yu, H., Nitrogen and sulfur co-doped graphene/carbon nanotube as metal-free electrocatalyst for oxygen evolution reaction: the enhanced performance by sulfur doping. *Electrochim. Acta* **2016,** 204, 169-175.
17.Zhang, J.; Dai, L., Nitrogen, Phosphorus, and Fluorine Tri-doped Graphene as a Multifunctional Catalyst for Self-Powered Electrochemical Water Splitting. *Angew. Chem. Int. Ed. Engl.* **2016,** 55, (42), 13296-13300.
18.Salas, E. C.; Sun, Z.; Lüttge, A.; Tour, J. M., Reduction of Graphene Oxide via Bacterial Respiration. *ACS Nano* **2010,** 4, (8), 4852-4856.
19.Jiao, Y.; Qian, F.; Li, Y.; Wang, G.; Saltikov, C. W.; Gralnick, J. A., Deciphering the Electron Transport Pathway for Graphene Oxide Reduction by Shewanella oneidensis MR-1. *J. Bacteriol.* **2011,** 193, (14), 3662-3665.

20.Liu, T.; Jiang, L.-L.; He, M.-F.; Zhu, Z.; Wang, D.-b.; Song, T.-S.; Tan, W.-m.; Ouyang, P.; Xie, J., Green synthesis of reduced graphene oxide by a GRAS strain Bacillus subtilis 168 with high biocompatibility to zebrafish embryos. *RSC Adv.* **2015,** 5, (74), 60024-60032.

21.Rathinam, N. K.; Berchmans, S.; Sani, R. K.; Salem, D. R., Rewiring the microbe-electrode interfaces with biologically reduced graphene oxide for improved bioelectrocatalysis. *Bioresour. Technol.* **2018,** 256, 195-200.

22.Song, T.-S.; Tan, W.-M.; Xie, J., Bio-Reduction of Graphene Oxide Using Sulfate-Reducing Bacteria and Its Implication on Anti-Biocorrosion. *Journal of Nanoscience and Nanotechnology* **2018,** 18, (8), 5770-5776.

23.Yoshida, N.; Miyata, Y.; Mugita, A.; Iida, K., Electricity Recovery from Municipal Sewage Wastewater Using a Hydrogel Complex Composed of Microbially Reduced Graphene Oxide and Sludge. *Materials* **2016,** 9, (9), 742.

24.Yoshida, N.; Miyata, Y.; Doi, K.; Goto, Y.; Nagao, Y.; Tero, R.; Hiraishi, A., Graphene oxide-dependent growth and self-aggregation into a hydrogel complex of exoelectrogenic bacteria. *Sci. Rep.* **2016,** 6, 21867.

25.Wei, L.; Karahan, H. E.; Goh, K.; Jiang, W.; Yu, D.; Birer, Ö.; Jiang, R.; Chen, Y., A high-performance metal-free hydrogen-evolution reaction electrocatalyst from bacterium derived carbon. *J. Mater. Chem. A* **2015,** 3, (14), 7210-7214.

26.Zhou, L.; Fu, P.; Wang, Y.; Sun, L.; Yuan, Y., Microbe-engaged synthesis of carbon dot-decorated reduced graphene oxide as high-performance oxygen reduction catalysts. *J. Mater. Chem. A* **2016,** 4, (19), 7222-7229.

27.Malvankar, N. S.; Vargas, M.; Nevin, K. P.; Franks, A. E.; Leang, C.; Kim, B. C.; Inoue, K.; Mester, T.; Covalla, S. F.; Johnson, J. P.; Rotello, V. M.; Tuominen, M. T.; Lovley, D. R., Tunable metallic-like conductivity in microbial nanowire networks. *Nat Nanotechnol* **2011,** 6, (9), 573-9.

28.Kalathil, S.; Pant, D., Nanotechnology to rescue bacterial bidirectional extracellular electron transfer in bioelectrochemical systems. *RSC Adv.* **2016,** 6, (36), 30582-30597.

29.Malvankar, N. S.; Lovley, D. R., Microbial nanowires: a new paradigm for biological electron transfer and bioelectronics. *ChemSusChem* **2012,** 5, (6), 1039-46.

30.Kumar, A.; Hsu, L. H.-H.; Kavanagh, P.; Barrière, F.; Lens, P. N. L.; Lapinsonnière, L.; Lienhard V, J. H.; Schröder, U.; Jiang, X.; Leech, D., The ins and outs of microorganism–electrode electron transfer reactions. *Nat. Rev. Chem.* **2017,** 1, 0024.

31.Estevez-Canales, M.; Kuzume, A.; Borjas, Z.; Füeg, M.; Lovley, D.; Wandlowski, T.; Esteve-Núñez, A., A severe reduction in the cytochrome C content of Geobacter sulfurreducens eliminates its capacity for extracellular electron transfer. *Environ. Microbiol. Rep.* **2015,** 7, (2), 219-226.

32.Busalmen, J. P.; Esteve-Nunez, A.; Berna, A.; Feliu, J. M., C-type cytochromes wire electricity-producing bacteria to electrodes. *Angew. Chem. Int. Ed. Engl.* **2008,** 47, (26), 4874-7.

33.Hunter, B. M.; Thompson, N. B.; Müller, A. M.; Rossman, G. R.; Hill, M. G.; Winkler, J. R.; Gray, H. B., Trapping an Iron(VI) Water-Splitting Intermediate in Nonaqueous Media. *Joule* **2018,** 2, (4), 747-763.

34.Holmes, D. E.; Mester, T.; O'Neil, R. A.; Perpetua, L. A.; Larrahondo, M. J.; Glaven, R.; Sharma, M. L.; Ward, J. E.; Nevin, K. P.; Lovley, D. R., Genes for two multicopper proteins required for Fe(III) oxide reduction in Geobacter sulfurreducens have different expression patterns both in the subsurface and on energy-harvesting electrodes. *Microbiology* **2008,** 154, (Pt 5), 1422-35.

35.Marcano, D. C.; Kosynkin, D. V.; Berlin, J. M.; Sinitskii, A.; Sun, Z.; Slesarev, A.; Alemany, L. B.; Lu, W.; Tour, J. M., Improved Synthesis of Graphene Oxide. *ACS Nano* **2010,** 4, (8), 4806-4814.

36.Alazmi, A.; Rasul, S.; Patole, S. P.; Costa, P. M. F. J., Comparative study of synthesis and reduction methods for graphene oxide. *Polyhedron* **2016,** 116, 153-161.

37.Bond, D. R.; Lovley, D. R., Electricity Production by Geobacter sulfurreducens Attached to Electrodes. *Appl. Environ. Microbiol.* **2003,** 69, (3), 1548-1555.

38.Lin, W. C.; Coppi, M. V.; Lovley, D. R., Geobacter sulfurreducens Can Grow with Oxygen as a Terminal Electron Acceptor. *Appl. Environ. Microbiol.* **2004,** 70, (4), 2525-2528.

39.Bansal, R.; Helmus, R. A.; Stanley, B. A.; Zhu, J.; Liermann, L. J.; Brantley, S. L.; Tien, M., Survival During Long-Term Starvation: Global Proteomics Analysis of Geobacter sulfurreducens under Prolonged Electron-Acceptor Limitation. *J. Proteome Res.* **2013,** 12, (10), 4316-4326.

40.Estevez-Canales, M.; Kuzume, A.; Borjas, Z.; Fueg, M.; Lovley, D.; Wandlowski, T.; Esteve-Nunez, A., A severe reduction in the cytochrome C content of Geobacter sulfurreducens eliminates its capacity for extracellular electron transfer. *Environ Microbiol Rep* **2015,** 7, (2), 219-26.

41.Krishnamoorthy, K.; Veerapandian, M.; Yun, K.; Kim, S. J., The chemical and structural analysis of graphene oxide with different degrees of oxidation. *Carbon* **2013,** 53, 38-49.

42.Pimenta, M. A.; Dresselhaus, G.; Dresselhaus, M. S.; Cançado, L. G.; Jorio, A.; Saito, R., Studying disorder in graphite-based systems by Raman spectroscopy. *PCCP* **2007,** 9, (11), 1276-1290.

43.Gangadharan, P. K.; Unni, S. M.; Kumar, N.; Ghosh, P.; Kurungot, S., Nitrogen-Doped Graphene with a Three-Dimensional Architecture Assisted by Carbon Nitride Tetrapods as an Efficient Metal-Free Electrocatalyst for Hydrogen Evolution. *CHEMELECTROCHEM* **2017,** 4, (10), 2643-2652.

44.Zhao, Y.; Nakamura, R.; Kamiya, K.; Nakanishi, S.; Hashimoto, K., Nitrogen-doped carbon nanomaterials as non-metal electrocatalysts for water oxidation. *Nat Commun* **2013,** 4, 2390.

45.Yu, X.; Zhang, M.; Chen, J.; Li, Y.; Shi, G., Nitrogen and Sulfur Codoped Graphite Foam as a Self-Supported Metal-Free Electrocatalytic Electrode for Water Oxidation. *Adv. Energy Mater.* **2016,** 6, (2).

46.Liu, M.; Zhang, R.; Chen, W., Graphene-supported nanoelectrocatalysts for fuel cells: synthesis, properties, and applications. *Chem. Rev.* **2014,** 114, (10), 5117-60.

47.Suen, N.-T.; Hung, S.-F.; Quan, Q.; Zhang, N.; Xu, Y.-J.; Chen, H. M., Electrocatalysis for the oxygen evolution reaction: recent development and future perspectives. *Chem. Soc. Rev.* **2017,** 46, (2), 337-365.

48.Zhou, H.; Yu, F.; Sun, J.; He, R.; Chen, S.; Chu, C.-W.; Ren, Z., Highly active catalyst derived from a 3D foam of Fe(PO₃)₂/Ni₂P for extremely efficient water oxidation. *Proceedings of the National Academy of Sciences* **2017,** 114, (22), 5607-5611.

49.Wang, L.; Xiao, F.-S., The Importance of Catalyst Wettability. *ChemCatChem* **2014,** 6, (11), 3048-3052.

50.Li, Y.; Zhao, C., Enhancing Water Oxidation Catalysis on a Synergistic Phosphorylated NiFe Hydroxide by Adjusting Catalyst Wettability. *ACS Catal.* **2017,** 7, (4), 2535-2541.

51.Zhou, J.; Lian, J.; Hou, L.; Zhang, J.; Gou, H.; Xia, M.; Zhao, Y.; Strobel, T. A.; Tao, L.; Gao, F., Ultrahigh volumetric capacitance and cyclic stability of fluorine and nitrogen co-doped carbon microspheres. *Nat Commun* **2015,** 6, 8503.

Table of contents